



# Numerical approach for stagnation point flow of Sutterby fluid impinging to Cattaneo–Christov heat flux model

EHTSHAM AZHAR\*, Z IQBAL, S IJAZ and E N MARAJ

Department of Mathematics, Faculty of Sciences, HITEC University, Taxila 44700, Pakistan

\*Corresponding author. E-mail: ehtsham@uaar.edu.pk

MS received 23 September 2017; revised 27 February 2018; accepted 10 April 2018;  
published online 6 September 2018

**Abstract.** The present study examines the stagnation point flow of a non-Newtonian fluid along with the Cattaneo–Christov heat flux model. The coupled system is simplified using suitable similar solutions and solved numerically by incorporating the shooting method with the Runge–Kutta of order five. The motivation is to analyse the heat transfer using an amended form of Fourier law of heat conduction known as the Cattaneo–Christov heat flux model. The influences of significant parameters are taken into the account. The computed results of velocity and temperature profiles are displayed by means of graphs. The notable findings are as follows. The viscous and thermal boundary layer exhibits opposite trends for Reynolds number, Deborah number and power-law index. The shear stress at the wall displays reverse patterns for shear thinning and shear thickening fluids. The Prandtl number contributes to increasing the Nusselt number while the Deborah number of heat flux plays the role of reducing it.

**Keywords.** Sutterby fluid; Cattaneo–Christov heat flux; stagnation point; nonlinear analysis; numerical solutions.

**PACS Nos** 44.25.+f; 47.10.ad; 47.50.–d

## 1. Introduction

Heat transfer mechanism plays a vital role in cooling nuclear reactors, magnetic drug targeting, heat conduction in tissues, thermal managing of electronic devices, etc. This mechanism is mostly illustrated by traditional Fourier law of heat conduction [1], which has a major drawback of measuring initial disturbance instantly throughout the whole medium, mainly due to the reason that the Fourier law establishes a parabolic relation for temperature profile. Cattaneo [2] upgraded the law of heat conduction by incorporating a thermal relaxation term, causing heat transformation in the form of thermal waves. Christov [3] included Oldroyd's upper convected derivatives in place of time derivative to bring about material invariant formulation. His work is termed as Cattaneo–Christov heat flux model. The heat transfer of Maxwell fluid slip flow in light of Cattaneo–Christov model is examined by Han *et al* [4]. A study on rotating upper convected Maxwell fluid flow is carried out by Mustafa [5]. Some recent attempts were also made in [6,7]. Furthermore, numerous non-Newtonian fluids are encountered in biological, industrial and engineering processes. Due to the wide range of applications of such fluids, much

emphasis has been placed on studying rheological properties of non-Newtonian fluids. Navier–Stokes constitutive equation is insufficient to describe the behaviour of complex fluids such as oil, suspended liquids, polymer melts, gasoline, paints, etc. The power-law fluid models have been playing a significant role in investigating the rheological properties of such fluids. Recently, the Sutterby fluid model [8,9] has been in the limelight because of its much compact mathematical structure and the ability to demonstrate properties of pseudoplastic as well as dilatant fluids. Boundary layer flow is observed in many industrial applications such as synthetic sheets extrusion, liquid films, metallic plate condensation, glass manufacture, etc. Sakiadis [10] first studied the phenomenon of stretching flow. Later on, numerous researchers have investigated various aspects of stretching flows. For example, Cortell [11] and Chakrabarti and Gupta [12] have acquired similarity solution and investigated the hydromagnetic flow and heat transfer effects over an extended stratum. Their work was extended to power-law fluid by Andersson *et al* [13]. In paper production, glass blowing and continuous casting, stagnation point flow and heat transfer are discerned. Viscous fluid stagnation point flow towards linear enlarging surface was explored by Chiam [14]. Ishak *et al* [15]

inspected the blended convection stagnant point flow towards a vertical permeable stretching sheet. Thermodynamic analysis in stagnation point flow towards a stretching surface is carried out by Mahapatra and Gupta [16]. Recently, Oahimirea and Olajuwonb [17] studied variable thermal conductivity for hydromagnetic flow near a stagnation point on a stretching sheet with heat source/sink. Axisymmetric gyratory stagnation point flow imposed on a radially stretching sheet was studied by Weidman [18]. Vajravelu *et al* [19] investigated the influence of Hall current on magnetohydrodynamics (MHD) flow and heat transfer above a slender stretching sheet in the presence of variable fluid properties. A study of nanofluids over a nonlinear stretching/shrinking shear was carried out by Pal *et al* [20]. Recently, Iqbal *et al* [21] examined the phenomena of transport of carbon nanotubes and bioconvection nanoparticles on stagnation point flow in the presence of induced magnetic field. Some new contributions in this regard are given in [22–27].

Motivated by the above-mentioned attempts, this paper focusses on the study of heat transfer by incorporating Cattaneo–Christov heat flux model of non-Newtonian fluid. Sutterby fluid model has been opted to examine rheological characteristics of shear thinning, shear thickening and Newtonian fluids. The present analysis may be beneficial for academic research in the field of heat transfer and industry.

## 2. Physical description and governing model

We consider the two-dimensional flow of Sutterby fluid bounded by stagnation point flow towards the stretching sheet. The  $x$ -axis is taken along the stretching surface in the direction of motion and the  $y$ -axis is perpendicular to it. In addition,  $U_e(x) = cx$  denotes the free stream velocity while  $u_w(x) = ax$  is the velocity of the stretching sheet, where  $a$  and  $c$  are positive constants. At the boundary, the temperature  $T$  takes constant values  $T_w$  and the ambient value of  $T$  is  $T_\infty$ . The physical flow phenomenon for both stretching and boundary layer flows is given in figure 1.

According to Azhar *et al* [28], the conservation of mass and momentum equations for incompressible Sutterby fluid can be expressed as

$$\frac{\partial u}{\partial x} + \frac{\partial v}{\partial y} = 0, \quad (1)$$

$$u \frac{\partial u}{\partial x} + v \frac{\partial u}{\partial y} = U_e \frac{\partial U_e}{\partial x} + \frac{\mu_0}{\rho} \frac{\partial}{\partial y} \left[ \frac{\partial u}{\partial y} + \frac{mB^2}{3} \left( \frac{\partial u}{\partial y} \right)^3 \right] \quad (2)$$

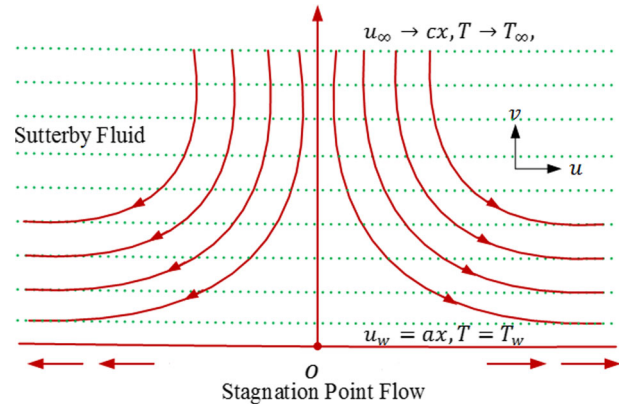


Figure 1. Engineering flow diagram.

with the related boundary conditions

$$u = u_w(x) = ax, \quad v = 0 \quad \text{at } y = 0, \\ u = U_e(x) = cx, \quad \frac{\partial u}{\partial y} \rightarrow 0 \quad \text{as } y \rightarrow \infty, \quad (3)$$

where  $u$  and  $v$  are the velocity components in the  $x$  and  $y$  directions, respectively,  $\rho$  is the fluid density,  $\mu_0$  is the viscosity,  $B$  is the material constant and  $m$  is the power-law index. Here  $m > 0$  represents the shear thickening or dilatant fluid,  $m < 0$  corresponds to the shear thinning or pseudoplastic fluid and for  $m = 0$ , the fluid is simply a Newtonian fluid. Several fluids can be studied by using different values of power-law index. Furthermore, the Cattaneo–Christov heat flux model (see [3,6]) can be expressed as

$$q + \lambda_3 \left( \frac{\partial q}{\partial t} + V \cdot \nabla q - q \cdot \nabla V - (\nabla \cdot V) q \right) = -k \nabla T, \quad (4)$$

in which  $q$  is the heat flux,  $\lambda_3$  is the relaxation time of heat flux,  $k$  is the thermal conductivity and  $V$  is the velocity vector. In view of the above expression, the energy equation can be written as

$$u \frac{\partial T}{\partial x} + v \frac{\partial T}{\partial y} + \lambda_3 \left( u \frac{\partial u}{\partial x} \frac{\partial T}{\partial x} + v \frac{\partial v}{\partial y} \frac{\partial T}{\partial y} + u \frac{\partial v}{\partial x} \frac{\partial T}{\partial y} + v \frac{\partial u}{\partial y} \frac{\partial T}{\partial x} + 2uv \frac{\partial^2 T}{\partial x \partial y} + u^2 \frac{\partial^2 T}{\partial x^2} + v^2 \frac{\partial^2 T}{\partial y^2} \right) = \alpha \frac{\partial^2 T}{\partial y^2} \quad (5)$$

with the relevant boundary conditions

$$T = T_w \text{ at } y = 0, \quad T \rightarrow T_\infty \text{ as } y \rightarrow \infty. \quad (6)$$

To further facilitate the present analysis, we introduce the subsequent conventional similarity transformation and dimensionless variable  $\eta$  and  $f(\eta)$  as

$$u = axf'(\eta), \quad v = -\sqrt{av}f(\eta), \quad \eta = y\sqrt{\frac{a}{v}},$$

$$\theta(\eta) = \frac{T - T_w}{T_\infty - T_w}. \quad (7)$$

In view of the similarity transformation (7), eq. (1) is identically satisfied and eqs (2)–(6) are reduced to the following form:

$$f''' + ff'' - f'^2 + \frac{m}{2} \text{Re De } f''^2 f''' + A^2 = 0, \quad (8)$$

$$\theta'' + \text{Pr } f\theta' - \text{Pr } \gamma(ff'\theta' + f^2\theta'') = 0 \quad (9)$$

with the associated boundary conditions

$$f(\eta) = 0, \quad f'(\eta) = 1, \quad \theta(\eta) = 1 \text{ at } \eta = 0,$$

$$f'(\eta) \rightarrow A, \quad \theta(\eta) \rightarrow 0 \text{ as } \eta \rightarrow \infty, \quad (10)$$

where prime represents the differentiation with respect to  $\eta$ , Re is the Reynolds number, De is the Deborah number, Pr is the Prandtl number and  $\gamma$  is the Deborah number with respect to heat flux. Moreover, the definition of these physical dimensionless parameters is

$$\text{Re} = \frac{ax^2}{v}, \quad \text{De} = B^2a^2, \quad A = \frac{c}{a}, \quad \gamma = \lambda_3a,$$

$$\text{Pr} = \frac{v}{\alpha}. \quad (11)$$

The physical quantity of interest such as skin friction coefficient  $C_f$  is given by

$$C_f = \frac{\tau_w}{\rho u_e^2(x)} \quad (12)$$

or

$$-\text{Re}_x^{1/2} C_f = \left[ f''(0) + \frac{m}{6} \text{De Re } (f''(0))^3 \right], \quad (13)$$

where  $\text{Re}_x = ax^2/v$  is the local Reynolds number based on the stretching velocity  $u_w(x)$ .

### 3. Computational methodology

This section includes shooting method along with the Runge–Kutta fifth-order technique to tackle the system of nonlinear differential equations. Thus, the solution of coupled nonlinear governing boundary layer eqs (8) and (9) together with boundary conditions (10) is computed by means of the shooting method along with the Runge–Kutta fifth-order technique. Initially, higher-order nonlinear differential equations expressed

in (8) and (9) are converted into a system of first-order differential equations and further transformed into an initial value problem by labelling the variables as  $(f, f', f'', \theta, \theta')^T = (y_1, y_1' = y_2, y_2' = y_3, y_4, y_4' = y_5)^T$ . According to our numerical procedure, the above system of equations is formulated as

$$\begin{pmatrix} y_1' \\ y_2' \\ y_3' \\ y_4' \\ y_5' \end{pmatrix} = \begin{pmatrix} y_2 \\ y_3 \\ \frac{2}{2 - m\text{ReDe}y_3^2}(y_2^2 - y_1y_3 - A^2) \\ y_5 \\ \text{Pr } y_1y_5/(1 - \text{Pr } \gamma y_1^2) \end{pmatrix}, \quad (14)$$

$$\begin{pmatrix} y_1(0) \\ y_2(0) \\ y_3(0) \\ y_4(0) \\ y_5(0) \end{pmatrix} = \begin{pmatrix} 0 \\ 1 \\ U_1 \\ 1 \\ U_2 \end{pmatrix}. \quad (15)$$

Appropriate values of unknown initial conditions  $U_1$  and  $U_2$  are approximated using Newton's method until the boundary conditions  $f'(\eta) \rightarrow 1 - \lambda$  and  $\theta(\eta) \rightarrow 0$  as  $\eta \rightarrow \infty$  are satisfied. Computations are carried out using the mathematics software MATLAB. End of a boundary layer region, i.e. when  $\eta = \infty$  to each group of parameters is determined, when the values of unknown boundary conditions at  $y = 1$  do not change to a successful loop with error less than  $10^{-6}$ .

### 4. Description of the results

In this section, variation of several emerging parameters for velocity and temperature profiles is displayed and examined. Figure 2 is drawn to examine the influence of velocity ratio parameter  $A$  ( $= (U_\infty/U_w)$ )

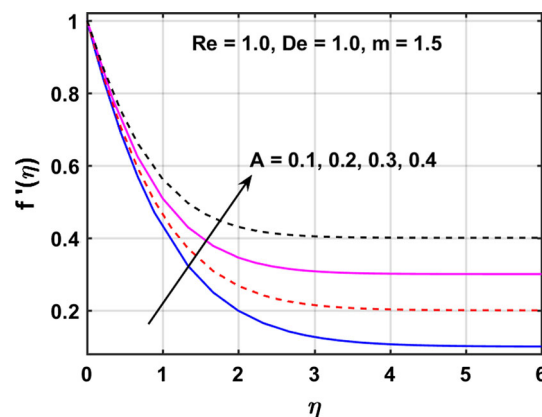


Figure 2. Variation of  $A$  with  $f'(\eta)$ .

on dimensionless velocity field  $f'(\eta)$ . For small values of  $A$  ( $0 < A < 1$ ), i.e. when the stretching velocity of a surface is greater than the stagnation velocity of the external stream, the viscous boundary layer thickness increases with an increase in  $A$ , where  $A = 1$  corresponds to a situation where the stretching velocity of a fluid is equal to the stagnation velocity of the external stream. Further, it is found that the flow has a boundary layer structure for values of  $A > 1$  and the boundary layer thickness decreases in this case. The contribution of power-law index  $m$  is shown in figure 3. For  $m < 0$  we can see the effect of a shear thinning fluid,  $m = 0$  is a Newtonian fluid and for  $m > 0$  the fluid shows a shear thickening behaviour. In figures 4 and 5, the velocity profiles are plotted for different values of Reynolds number  $Re$  for shear thickening and shear thinning fluids, respectively. From figure 4 it is clear that fluid velocity increases for high Reynolds number for shear thickening fluid ( $m > 0$ ), whereas in shear thinning case ( $m < 0$ ), for larger values of  $Re$ , the viscous forces decrease and as a result the fluid flow decelerates (see figure 5). The fluidity characteristic of a fluid is measured by Deborah number  $De$  under the specific

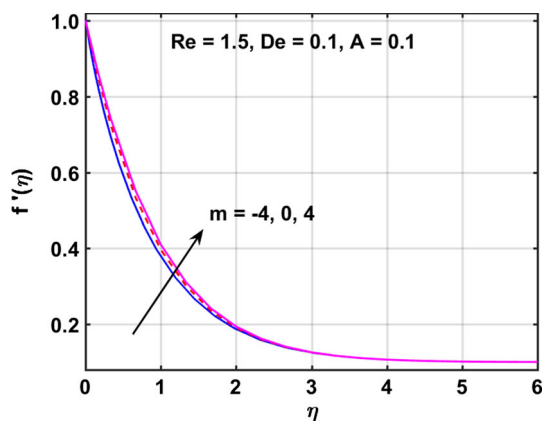


Figure 3. Variation of  $m$  with  $f'(\eta)$ .

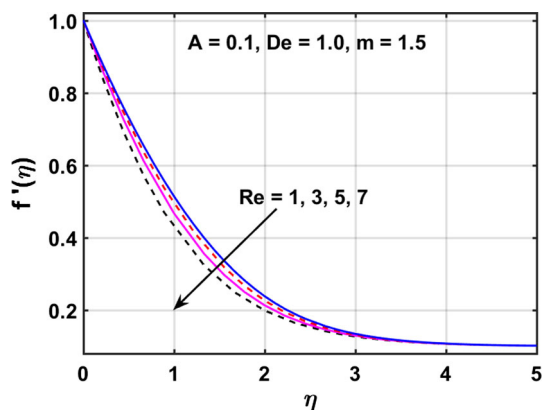


Figure 4. Variation of  $Re$  with  $f'(\eta)$  when  $m > 0$ .

flow condition. Deborah number  $De$  for  $m > 0$  and  $m < 0$  has quite opposite effects on the velocity of fluid. The fluid flow accelerates with an increase in  $De$  (see figure 6), but it decelerates for larger values of Deborah number in the case of a shear thinning fluid (see figure 7). The rise in  $De$  plays a role in improving elastic effects, which for dilatant fluids leads to improved fluid flow, while the opposite trend is witnessed for the pseudoplastic fluid.

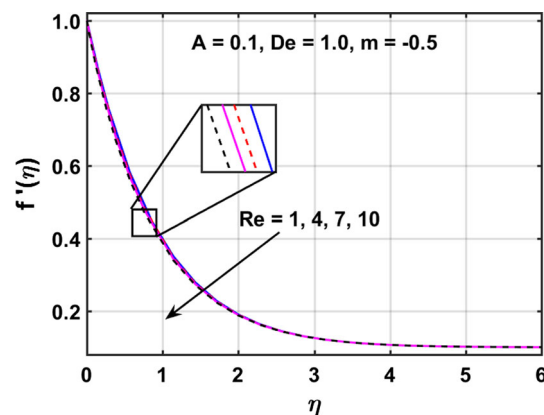


Figure 5. Variation of  $Re$  with  $f'(\eta)$  when  $m < 0$ .

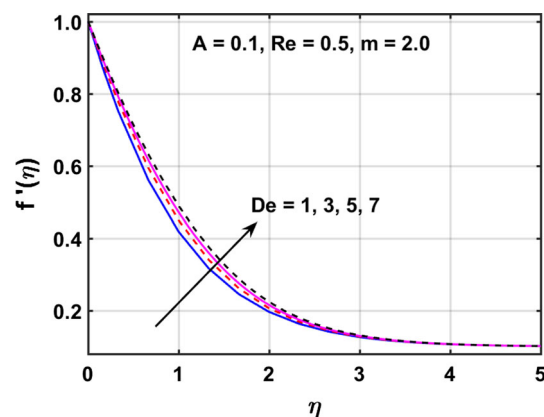


Figure 6. Variation of  $De$  with  $f'(\eta)$  when  $m > 0$ .

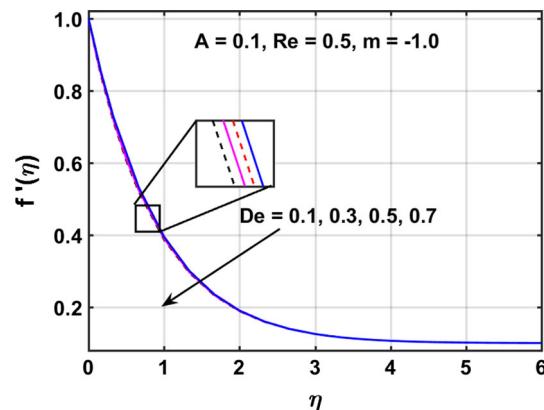
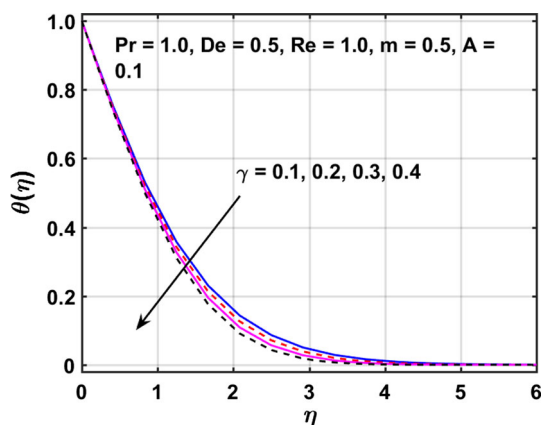
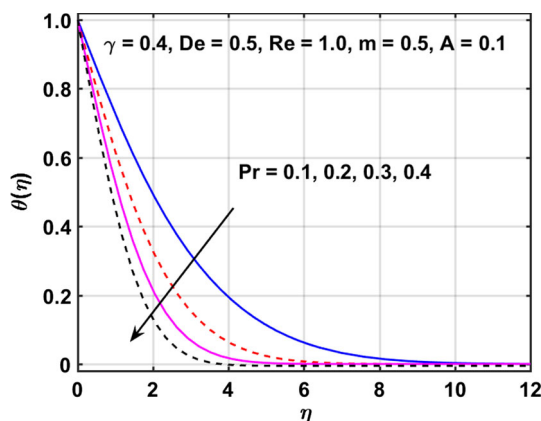


Figure 7. Variation of  $De$  with  $f'(\eta)$  when  $m < 0$ .

The effects of notable parameters on temperature profile  $\theta(\eta)$  are plotted in figures 8–13. Figure 8 shows that the temperature and thermal boundary layer thickness reduce for larger values of  $\gamma$ . The  $\gamma$  arises due to heat flux relaxation time. The fluid with greater relaxation time has lower temperature and the fluid with the smaller heat flux relaxation time corresponds to higher temperature. From figure 9 it is found that an increase in Prandtl number  $Pr$  decreases the fluid temperature  $\theta(\eta)$  and reduces the thermal boundary layer thickness because an increase in  $Pr$  decreases the thermal conductivity. Therefore, a higher Prandtl number fluid has a thinner thermal boundary layer. The contribution of  $A$  on temperature is shown in figure 10. An increase in  $A$  results in a decrease in temperature and thermal boundary thickness. Figure 11 indicates the contribution of power-law index  $m$  on  $\theta(\eta)$  for three classifications. Prominent temperature is observed for shear thinning fluids compared to the other two categories. Figures 12 and 13 show the effect of Deborah number  $De$  and Reynolds number  $Re$  on the temperature profile. From these figures it can be seen that the thermal



**Figure 8.** Variation of  $\gamma$  with  $\theta(\eta)$ .



**Figure 9.** Variation of  $Pr$  with  $\theta(\eta)$ .

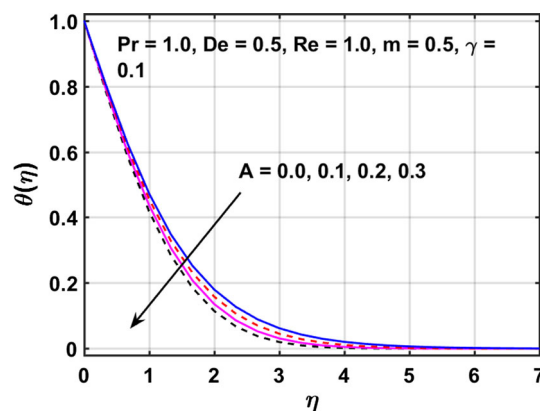


**Figure 10.** Variation of  $A$  with  $\theta(\eta)$ .

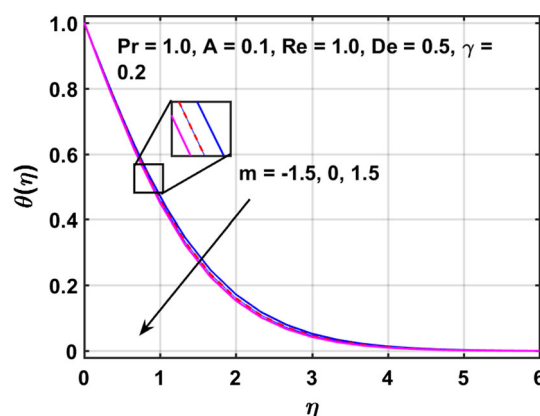


**Figure 11.** Variation of  $m$  with  $\theta(\eta)$ .

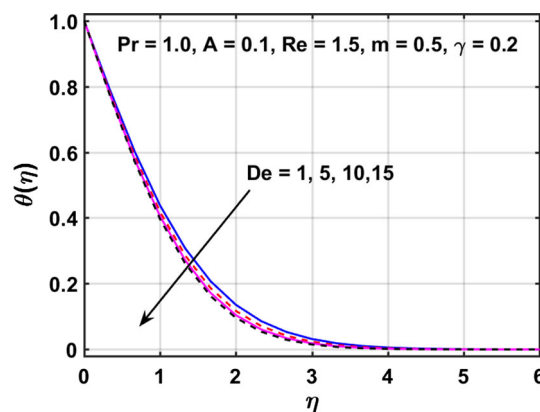


**Figure 12.** Variation of  $De$  with  $\theta(\eta)$ .

boundary layer thickness decreases with the increase in Deborah number and Reynolds number. In the case of dilatant fluids, an increase in  $Re$  and  $De$  plays a role in increasing the viscous forces and elastic forces, respectively, which leads to an enhancement in viscous boundary layer, affecting the thermal boundary layer by reducing it.



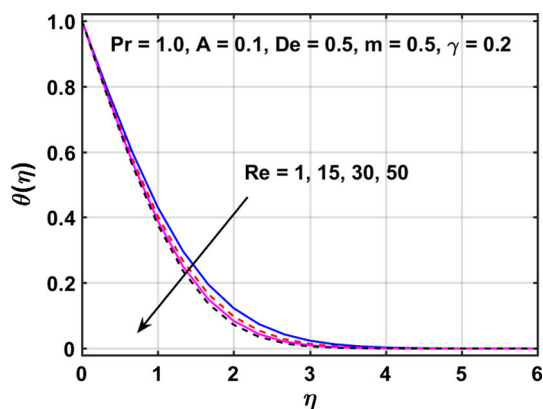


**Figure 13.** Variation of  $Re$  with  $\theta(\eta)$ .

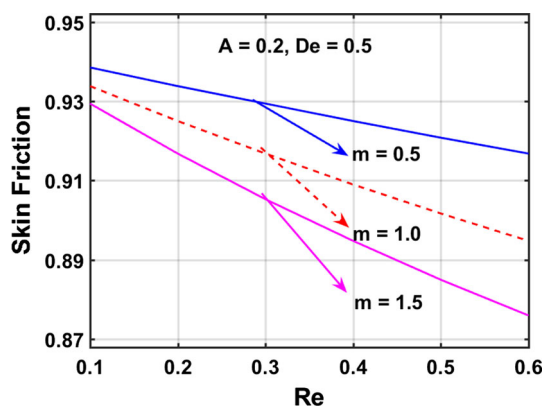


**Figure 14.** Variation of  $Re$  with  $m$  when  $m > 0$ .

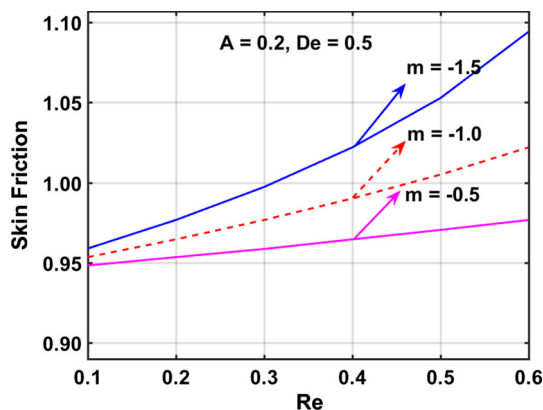


**Figure 15.** Variation of  $Re$  with  $m$  when  $m < 0$ .

The numerical values of skin friction coefficient against different parameters have been demonstrated in figures 14–18. Figures 14 and 15 show plots of skin friction against the Reynolds number  $Re$  for shear thickening and thinning fluids, respectively. For  $m > 0$ , the rising Reynolds number reduces skin friction and an opposite behaviour is depicted for  $m < 0$ . The Deborah number also has the same impact on computation values of skin friction, i.e. it decreases with higher values

of  $De$  for dilatant (see figure 16) and increases for the corresponding Deborah number in the case of pseudoplastic fluids for fixed values of  $A$  and  $Re$  (see figure 17). The variation of stretching parameter against  $m < 0$ ,  $m = 0$  and  $m > 0$  for skin friction is plotted in figure 18. The numerical values for a Newtonian fluid lie between the dilatant and pseudoplastic fluids.

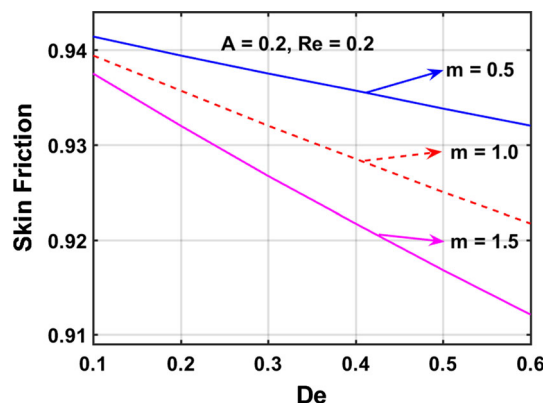


**Figure 16.** Variation of  $De$  with  $m$  when  $m > 0$ .

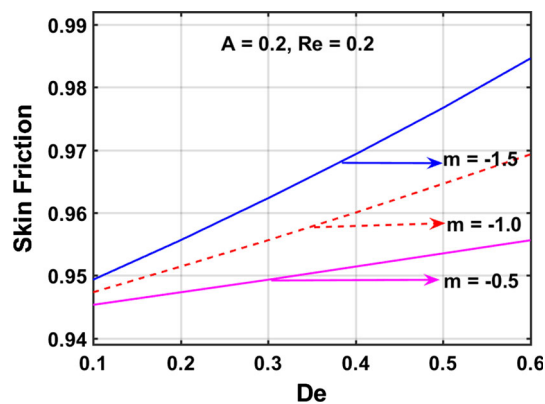


**Figure 17.** Variation of  $De$  with  $m$  when  $m < 0$ .

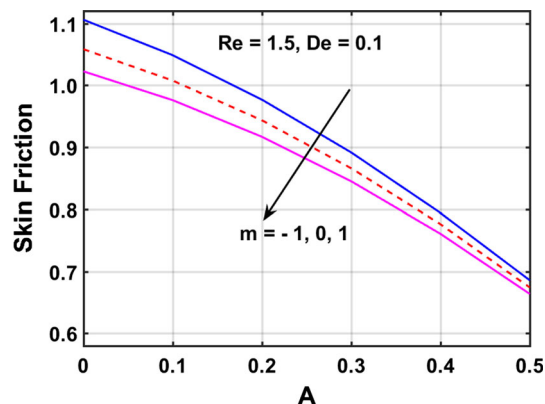


**Figure 18.** Variation of  $A$  with  $m$ .

## 5. Concluding remarks

This paper focussed on studying heat transfer of Sutterby fluid using the Cattaneo–Chistov heat flux model. Numerical solution for a two-dimensional flow problem towards a stretching sheet was carried out by means of shooting algorithm after the utilisation of similarity analysis. Numerical results were obtained which are correct up to six decimal places. The key findings of the present analysis are: hydrodynamic boundary layer flow is linear for  $A = 1$ , for  $A > 1$  the fluid velocity increases and for  $A < 1$  it decreases. The velocity field increases while the temperature profile decreases as the Reynolds number  $Re$  and Deborah number  $De$  increase for shear thickening fluids. The power-law index  $m$  has quite opposite effects on the dimensionless temperature and fluid velocity for increasing values of  $Pr$  and  $\gamma$  lead to a reduction in the temperature profile and thermal boundary layer thickness. For shear thickening fluid, the numerical values of skin friction decrease for larger  $Re$  and  $De$  while they increase for a shear thinning case. The Nusselt number decreases as  $\gamma$  increases and the enhancement can be observed for higher Prandtl number. The rate of heat flux increases as  $Pr$  increases and a decay can be seen corresponding to  $\gamma$ . The novel results of the present analysis may be beneficial for academic research in the field of heat transfer and industry.

## References

- [1] J B J Fourier, *Theorie analytique de la chaleur* (Chez Firmin Didot, Paris, 1822)
- [2] C Cattaneo, Sulla conduzionedelcalore, in: *Atti del Seminario Matematico e Fisico dell Universita di Modena e Reggio Emilia*, Vol. 3, p. 83 (1948)
- [3] C I Christov, *Mech. Res. Commun.* **36**, 481 (2009)
- [4] S Han, L Zheng, C Li and X Zhang, *Appl. Math. Lett.* **38**, 87 (2014)
- [5] M Mustafa, *AIP Adv.* **5**, 047109 (2015)
- [6] E Azhar, Z Iqbal, E N Maraj and B Ahmad, *Front. Heat Mass Transf.* **8**, 22 (2017)
- [7] B Ahmad and Z Iqbal, *Front. Heat Mass Transf.* **8**, 25 (2017)
- [8] J L Sutterby, *AIChE J.* **12**, 63 (1966)
- [9] R L Batra and M Eissa, *Polym. Plast. Technol. Eng.* **33**, 489 (1994)
- [10] B C Sakiadis, *AIChE J.* **7**, 26 (1961)
- [11] R Cortell, *Int. J. Non Linear Mech.* **29**, 155 (1994)
- [12] A Chakrabarti and A S Gupta, *Q. Appl. Math.* **37**, 73 (1979)
- [13] H I Andersson, K H Bech and B S Dandapat, *Int. J. Non Linear Mech.* **27**, 929 (1992)
- [14] T C Chiam, *J. Phys. Soc. Jpn.* **63**, 2443 (1994)
- [15] A Ishak, R Nazar and I Pop, *Chem. Eng. J.* **148**, 63 (2009)
- [16] T R Mahapatra and A S Gupta, *Heat Mass Transf.* **28**, 517 (2002)
- [17] J I Oahimirea and B I Olajuwonb, *Int. J. Appl. Sci. Eng.* **11**, 331 (2013)
- [18] P Weidman, *Int. J. Non-Linear Mech.* **82**, 1 (2016)
- [19] K Vajravelu, K V Prasad and H Vaidya, *Commun. Numer. Anal.* **2016**, 17 (2016)
- [20] D Pal, G Mandal and K Vajravalu, *Commun. Numer. Anal.* **2015**, 30 (2015)
- [21] Z Iqbal, E N Maraj, E Azhar and Z Mehmood, *J. Taiwan Inst. Chem. Eng.* **81**, 150 (2017)
- [22] Z Iqbal, E Azhar and E N Maraj, *Phys. E: Low-Dimen. Syst. Nanostruct.* **91**, 128 (2017)
- [23] Z Iqbal, E N Maraj, E Azhar and Z Mehmood, *Adv. Powder Technol.* **28**, 2332 (2017)
- [24] E N Maraj, Z Iqbal, Z Mehmood and E Azhar, *Eur. Phys. J. Plus* **132**, 476 (2017)
- [25] Z Iqbal, Z Mehmood, E Azhar and E N Maraj, *J. Mol. Liq.* **234**, 296 (2017)
- [26] Z Iqbal, N S Akbar, E Azhar and E N Maraj, *Alex. Eng. J.*, <https://doi.org/10.1016/j.aej.2017.03.047> (2017)
- [27] Z Iqbal, N S Akbar, E Azhar and E N Maraj, *Eur. Phys. J. Plus* **132**, 143 (2017)
- [28] E Azhar, Z Iqbal and E N Maraj, *Z. Naturf. A* **71**, 837 (2016)